Eur. Phys. J. A **28**, 193–203 (2006)
DOI 10.1140/epja/i2006-10054-4

THE EUROPEAN PHYSICAL JOURNAL A

Excitation functions of evaporation residues in the interaction of ^{16}O with ^{103}Rh at incident energies up to 400 MeV

E.Z. Buthelezi[1], F. Cerutti[2], E. Gadioli[2,a], G.F. Steyn[1], A. Pepe[2], S.H. Connell[3], and A.A. Cowley[1,4]

[1] iThemba LABS, Somerset West, South Africa
[2] Department of Physics, Milan University and INFN, Italy
[3] School of Physics, Witwatersrand University, Johannesburg, South Africa
[4] Department of Physics, University of Stellenbosch, South Africa

Received: 8 March 2006 / Revised: 23 May 2006 /
Published online: 21 June 2006 –
Communicated by C. Signorini

Abstract. The excitation functions for production of 48 residues in the interaction of ^{16}O with ^{103}Rh have been measured at incident energies varying from about 40 to 400 MeV. Their analysis shows that many competing reaction mechanism contribute to the formation of these residues including complete fusion, break-up–fusion reactions and ^{16}O inelastic scattering. The cross-sections of most of these mechanisms are obtained by independent measurements of the spectra of intermediate-mass fragments observed in the interaction of ^{16}O on ^{93}Nb. The agreement between measured and calculated excitation functions is satisfactory in most of the cases.

PACS. 25.70.Gh Compound nucleus – 25.70.Mn Projectile and target fragmentation

1 Introduction

There is an increasing need for information on inclusive nuclear reactions induced both by light particles and heavy ions due to their relevance in interdisciplinary fields and applications. The data required for these purposes are the multiplicity and the spectra of the emitted particles and the intermediate-mass fragments (IMFs) which may be produced, the yield and the spectra of the *evaporation* residues and the γ, β and/or α particle spectra from the subsequent radioactive decay.

Reactions induced by light particles are better known both from an experimental and a theoretical point of view. The available information in this field has been reviewed in recent international conferences, see for instance [1], and in reports such as [2]. The knowledge in the case of heavy-ion reactions is much less systematic and often essential experimental information is lacking, even in the case of ions such as ^{12}C and ^{16}O, which are increasingly important in applications and interdisciplinary fields such as hadrontherapy [3] and space radiation protection [4].

A large variety of different mechanisms contribute to reactions induced by such ions even at rather low energies, originating both from their fusion with the target nucleus and their fragmentation which, as shown for instance in [5], occurs with sizeable cross-sections already at incident energies below 10 MeV/n. In a recent paper we have analysed the excitation functions for production of a large number of residues in the interaction of ^{12}C with ^{103}Rh from the Coulomb barrier up to incident energies of $\sim$ 35 MeV/n, which is a case that we consider to be representative of asymmetric reactions involving carbon ions in this energy range [6]. In this paper we discuss the reactions induced by ^{16}O on the same target nucleus at energies varying from the Coulomb barrier up to 25 MeV/n.

The analysis of these data as well as of complementary data, as will be discussed in sect. 2, leads one to recognize the presence of a fast stage of the interaction (up to a time of about 200 fm/c) in which fast light particles and IMFs are emitted leaving an excited intermediate nucleus in statistical equilibrium and a subsequent slow stage requiring to be completed times up to about 10^{-16} s, during which a statistical competition between the different decay modes of equilibrated nuclei occurs.

What happens in the fast stage may be studied in the case of asymmetric reactions by measuring the hardest part of the emitted light particle spectra and the spectra of IMFs, which are strongly suppressed once an equilibrated nucleus is created at the end of the fast stage. Recent experiments have suggested that the IMFs are produced both by projectile fragmentation and, with unexpectedly large cross-sections by nucleon coalescence during nuclear *thermalization*, the cascade of nucleon interac-

[a] e-mail: ettore.gadioli@mi.infn.it

tions through which the excited nuclei produced in the primary two-ion interaction reach statistical equilibrium [5, 7–9].

The slow stage of the reaction eventually leads to the production of residues which, though well separated in mass by the particles emitted in the fast stage of the reaction, may nevertheless have a considerably smaller mass than the target nucleus even at incident energies of only a few tens of MeV/n.

The fast stage of the reaction greatly biases the subsequent slow stage. The average excitation energy of the equilibrated nuclei left at the end of the fast stage is only a fraction of the initial energy, substantially reducing the number of particles which may subsequently evaporate.

As mentioned before, in this paper we present a comprehensive account of the reactions occurring in the interaction of ^{16}O with ^{103}Rh at incident energies up to about 25 MeV/n. We achieve that through the analysis of a large number of excitation functions for production of evaporation residues. However, as discussed later, this analysis alone is not sufficient to provide unambiguous conclusions and it needs to be accompanied by the simultaneous analysis of complementary data [6]. In the next section we will review this complementary information which we have obtained through the study of the spectra of particles emitted during the fast interaction stage. In sect. 3 the experimental procedures adopted for measuring the excitation functions are described. In sect. 4 the analysis of these data is presented and sect. 5 is devoted to the conclusions.

2 Review of independent data relevant to present investigation

Some years ago, for the interaction of ^{16}O with ^{165}Ho and ^{181}Ta at incident energies up to about 8 MeV/n, the excitation functions for production of evaporation residues and the forward range distributions of some of them were measured using the activation technique. The analysis of these data, summarized in [10], suggested that already at such low energies many different mechanisms contribute, such as the two-ion fusion and the incomplete fusion of fragments produced in ^{16}O binary fragmentation. The fragments considered in that work were ^{12}C, ^{8}Be, ^{6}Li and α particles. It was also possible to estimate the absolute cross-sections of the contributing mechanisms. The results obtained are summarized in fig. 5 of [10], which shows the measured reaction cross-section for the interaction of ^{12}C and ^{16}O ions with ^{181}Ta from an incident energy corresponding to the two-ion Coulomb barrier up to about 8 MeV/n, as well as the contributions of complete fusion and the already-mentioned incomplete-fusion processes.

These investigations revealed that for such heavy targets, the ratio of fission to the spallation reaction cross-section increases quite steeply with increasing incident ^{16}O energy, making it increasingly difficult to separate the contributing mechanisms. Consequently, in order to investigate how these contributions evolve with increasing energy, minimizing the contribution of fission, it was decided to study the interaction of ^{16}O with a lighter target nucleus. The nucleus ^{103}Rh was chosen for this purpose because of the favourable radioactive properties of an abundance of residues which could be produced in an activation measurement. The results of the experiment, which enabled us to measure the excitation functions for production of a large number of residues up to an incident energy of 25 MeV/n, are discussed in the next section of this paper.

In the course of this investigation we were soon convinced that, in order to reach unambiguous conclusions, the study of these data, which reflect the full complexity of the interaction, should be accompanied by the contemporary study of the processes occurring during the initial fast stage of the interaction. The data which eventually provided the more significant information are the spectra of the IMFs emitted in the interaction of ^{16}O with ^{93}Nb up to about 25 MeV/n [5,7]. The choice of this target nucleus was motivated by the fact that it was not possible to obtain self-supporting ^{103}Rh targets as required by this type of experiments and ^{93}Nb was considered sufficiently close to ^{103}Rh to enable the use of the information obtained in the analysis of the rhodium data. This presumption was confirmed by the similarity of the conclusions drawn from the analysis of the spectra of IMFs produced in the interaction of ^{16}O with ^{59}Co.

The analysis of these data showed that ^{16}O binary fragmentation greatly contributes to the measured IMF spectra and this process appears to be more complex than originally anticipated. Indeed, it is found that the average energy of the IMFs produced by binary fragmentation and the width of their spectra are smaller and wider, respectively, than those expected for a *quasielastic* fragmentation process. This may indicate that either the projectile, before fragmentation, or the observed fragment, after being produced, underwent a considerable energy exchange with the target or the residual nucleus, thus losing quite a significant amount of their energy. The results obtained in the analysis of the IMF spectra produced in the interaction of ^{12}C with the same nuclei led to the same conclusion and suggested the predominance of the initial-state interaction of the projectile as discussed in [8,9,11,12]. This assumption allowed a very reasonable reproduction also of the spectra of the IMF produced in the ^{16}O interaction [5,7].

An initial-state interaction appears indeed a very reasonable possibility since even in the more peripheral inelastic-scattering interaction, the projectile may lose quite a considerable amount of its energy. A simple way of accounting for these spectra was proposed by introducing a *projectile survival probability function* (PSPF) to mass exchange and break-up, which was assumed to exponentially decrease with increasing projectile energy loss (as suggested by the energy averaged spectra of the inelastically scattered ions), and folding the IMF spectra evaluated with the *local plane-wave approximation* (LPWA) proposed by [13,14] with the PSPF as discussed in [5,7, 11,12]. Another interesting observation was that ^{16}O (as

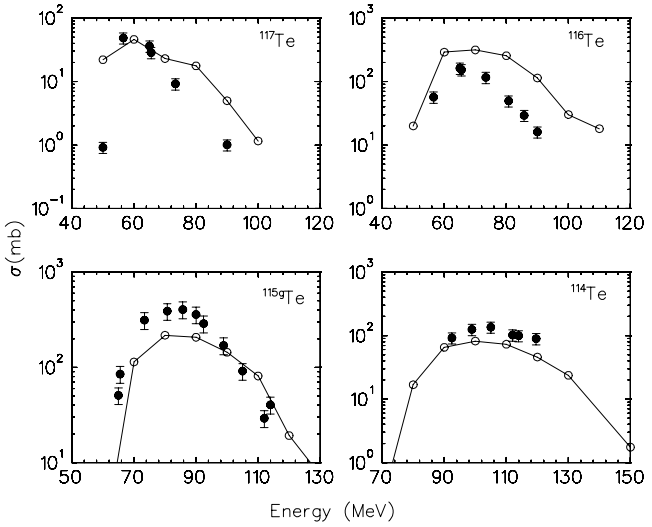

Fig. 1. Comparison of experimental (black dots) and calculated (full lines) excitation functions for production of Te isotopes. Here and in the following figures, up to fig. 11, the lines, which connect the calculated values (open dots) do not represent the true shape of the calculated excitation functions, especially in the region of the maxima, and are simply meant to visualize the trend of the calculated cross-sections.

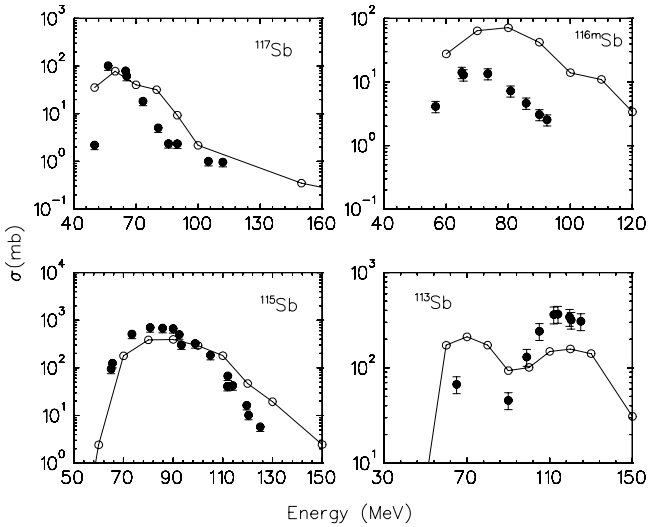

Fig. 2. Comparison of experimental (black dots) and calculated (open dots connected by the full lines) excitation functions for production of Sb isotopes.

was also found for ^{12}C [8,9]) may fragment in many different ways, a fact which was not clearly recognized before.

Another unexpected finding was that a considerable amount of IMFs with energy around the Coulomb barrier is produced in these interactions. The Boltzmann Master Equation (BME) theory, which we previously used to describe the cascade of nucleon-nucleon (n-n) interactions which lead to nuclear thermalization and the spectra of the light particles emitted in the course of this cascade [15,16], successfully reproduced this contribution to the measured IMF spectra. An example of the results obtained may be found in [5,7] where are shown the spectra of boron, carbon and nitrogen fragments produced in the interaction of ^{16}O with ^{93}Nb at incident energies varying from 100 to 400 MeV.

The analysis of the IMF spectra provided values for the fragmentation cross-sections, the average initial loss of energy of oxygen before fragmentation and other important computational parameters which are used as input for the excitation function calculations, as will be discussed in sect. 4.

3 Experimental procedure and results

We have measured by the activation technique the excitation functions for production of 48 residues with mass and charge varying, respectively, from 117 to 85 and 52 to 39 in the interaction of ^{16}O with ^{103}Rh at energies varying from about 40 up to 400 MeV. The ^{103}Rh targets were thin (310 μg/cm^2) foils deposited on a 1.5 μm thick mylar backing (provided by Goodfellow Cambridge Limited, Cambridge, England). The measurement of the induced activity in the target and a catcher in close contact with it started a few minutes after irradiation and lasted for several weeks.

At incident energies below $\sim$ 126 MeV the irradiations were made at the Laboratori Nazionali del Sud (LNS) in Catania, Italy. At energies ranging from $\sim$ 93 to 400 MeV the rhodium targets were irradiated at iThemba LABS (formerly the National Accelerator Centre) in Faure, Somerset West, South Africa.

At the LNS, two sets of irradiations were made: i) the first was made using single rhodium targets and thick aluminium catchers and consisted of 5 irradiations at energies varying from 50 to $\sim$ 112 MeV, ii) the second was made using the stacked-foil technique and consisted of 4 irradiations at energies of 57, 82, 100 and 126 MeV. In each irradiation the stack consisted of three rhodium targets interspaced by aluminium foils which acted as catchers and degraders.

In the irradiations performed at iThemba LABS we used stacked foils of 16 ^{103}Rh targets interspaced with aluminium foils acting as catchers and degraders. The rhodium targets were the same as before, *i.e.* 310 μg/cm^2 foils deposited on a 1.5 μm thick mylar backing. In total, three irradiations were performed at incident ^{16}O energies of 201.6, 294.8, and 398.5 MeV.

In all irradiations both at LNS and iThemba LABS the beam current was monitored every few seconds to allow one to account for possible fluctuations of beam intensity in evaluating the production cross-sections of the residues. Many tests were made for estimating the uncertainty of the measured time-integrated beam fluence which led to an estimated accuracy between 5 and 10%.

Both at LNS and iThemba LABS, the activities induced in the targets and catchers were measured with calibrated HPGe detectors. The residues were identified by their respective characteristic γ lines as well as their half-lives by measuring the decrease of the activity with time. Table 1 gives the list of the identified isotopes with mass

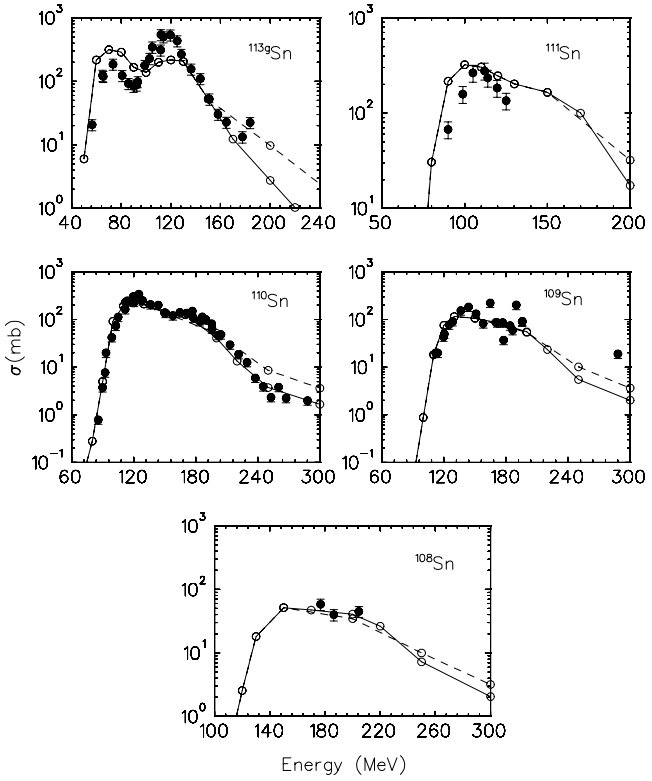

Fig. 3. Comparison of experimental (black dots) and calculated (open dots connected by the dashed and full lines) excitation functions for production of Sn isotopes. The assumptions underlying the two theoretical predictions are explained in the text.

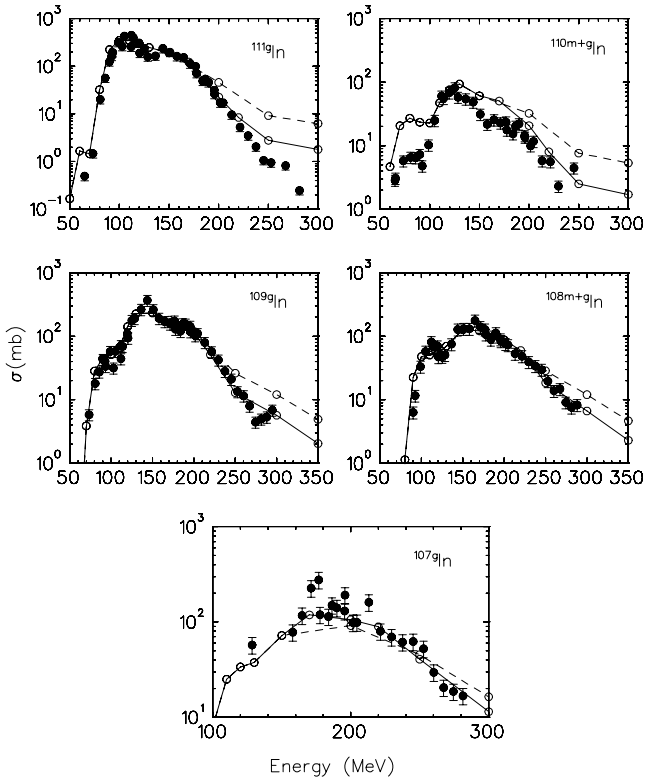

Fig. 4. Comparison of experimental (black dots) and calculated (open dots connected by the dashed and full lines) excitation functions for production of In isotopes. The assumptions underlying the two theoretical predictions are explained in the text.

Table 1. Identified isotopes with mass exceeding 113, their half-lives and spin, energies and abundances of characteristic γ lines. The corresponding information for lower-mass residues may be found in table 1 of ref. [6]

Isotope	Half-life (h)	J^π	E_γ (keV)	Abundance (%)	Reference
^{117}Te	1.033	$1/2^+$	719.7	65	[17]
^{116}Te	2.49	0^+	628.72	3.21	[18]
			1055.3	0.51	
^{115}Te	0.097	$7/2^+$	723.569	30	[19]
^{114}Te	0.253	0^+	726.9	7.35	[20]
			244.59	6.8	
			1417.4	6.06	
			479.56	5.47	
^{117}Sb	2.80	$5/2^+$	158.562	86	[21]
^{116}Sb	0.263	3^+	1293.558	84.8	[18]
^{115}Sb	0.535	$5/2^+$	497.358	98	[19]

higher than 113, their half-life and spin, the energy and abundance of the characteristic γ lines which were used. The corresponding information for lower-mass isotopes is given in table 1 of [6].

A residue may be produced both independently in the interaction of the two ions and by the decay of precursors which are also independently produced together with the residue of interest. If the residue is not chemically separated by its precursors, and its activity is measured at times much larger than the precursor half-lives, the cross-sections for formation of the precursors, multiplied by factors which depend on the branching for the decay of the precursors to the residue and on the half-lives of the precursors and residues, add to the independent formation cross-section of the residue to give a cumulative formation cross-section [22,23]. For residues with mass higher than 113, table 2 integrates the list of the cumulative cross-sections for formation of the observed residues as a func-

Table 2. Cumulative cross-sections for production of residues with mass exceeding 113. The corresponding information for lower-mass residues may be found in table 2 of ref. [6].

Residue	Contributions to its production
^{117}Te	$^{117}\mathrm{Te} + 1.038\,^{117}\mathrm{I}$
^{116}Te	$^{116}\mathrm{Te} + {}^{116}\mathrm{I}$
$^{115}\mathrm{Te}^{\mathrm{g}}$	$^{115}\mathrm{Te}^{\mathrm{g}} + 1.289\,^{115}\mathrm{I}$
$^{114}\mathrm{Te}^{\mathrm{g}}$	$^{114}\mathrm{Te}^{\mathrm{g}} + 1.002\,^{114}\mathrm{I}$
^{117}Sb	$^{117}\mathrm{Sb} + 1.582\,^{117}\mathrm{Te} + 1.604\,^{117}\mathrm{I}$
$^{116}\mathrm{Sb}^{\mathrm{m}}$	$^{116}\mathrm{Sb}^{\mathrm{m}}$
$^{116}\mathrm{Sb}^{\mathrm{g}}$	$^{116}\mathrm{Sb}^{\mathrm{g}} - 0.120(\,^{116}\mathrm{Te} + {}^{116}\mathrm{I})$
$^{115}\mathrm{Sb}^{\mathrm{g}}$	$^{115}\mathrm{Sb}^{\mathrm{g}} + 1.221\,^{115}\mathrm{Te}^{\mathrm{m}} + 1.265\,^{115}\mathrm{Te}^{\mathrm{g}} + 1.297\,^{115}\mathrm{I}$

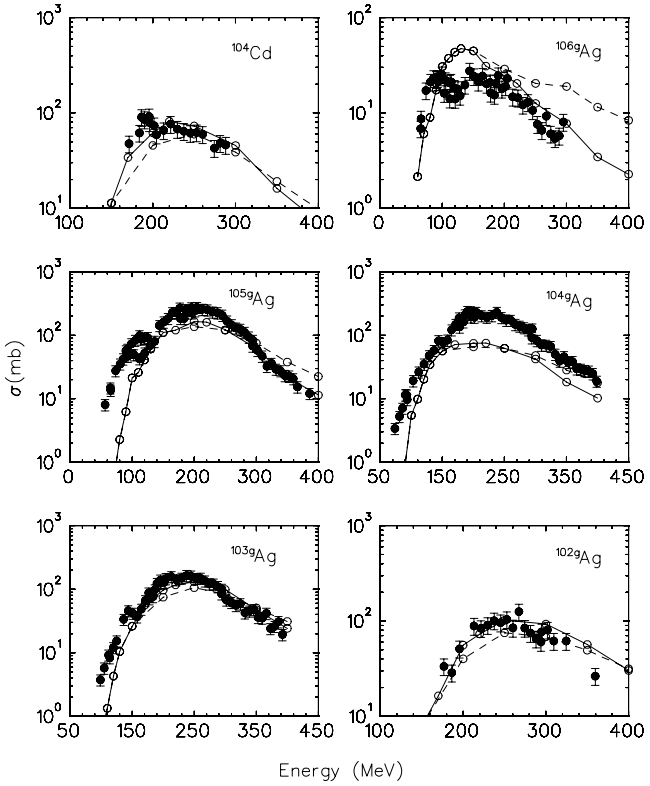

Fig. 5. Comparison of experimental (black dots) and calculated (open dots connected by the dashed and full lines) excitation functions for production of ^{104}Cd and Ag isotopes. The assumptions underlying the two theoretical predictions are explained in the text.

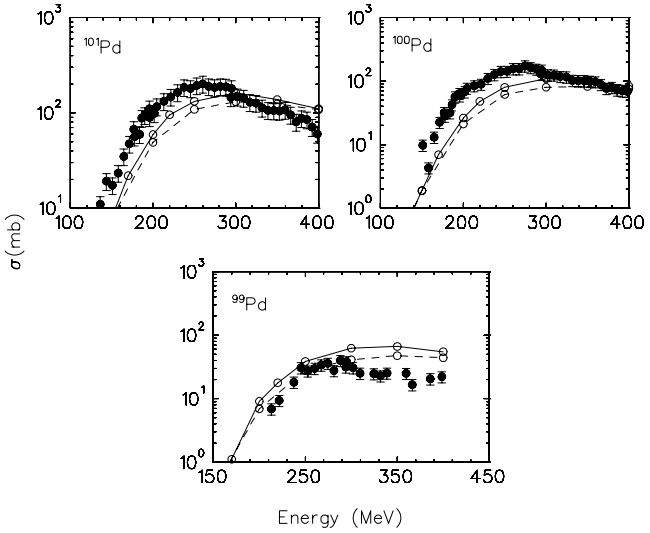

Fig. 6. Comparison of experimental (black dots) and calculated (open dots connected by the dashed and full lines) excitation functions for production of Pd isotopes. The assumptions underlying the two theoretical predictions are explained in the text.

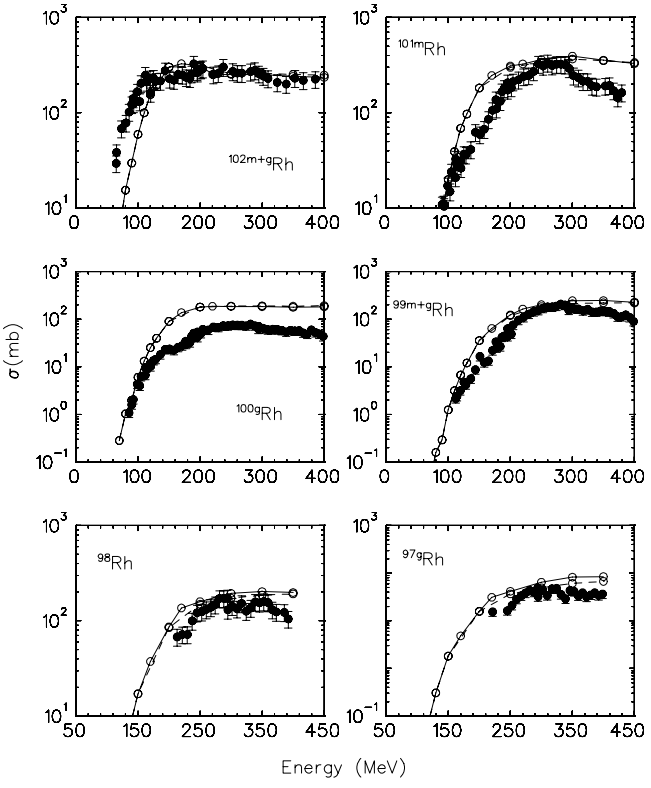

Fig. 7. Comparison of experimental (black dots) and calculated (open dots connected by the dashed and full lines) excitation functions for production of Rh isotopes. The assumptions underlying the two theoretical predictions are explained in the text.

tion of the residue and precursor independent production cross-sections, given in [6]. The experimental value of these cumulative cross-sections deduced from the known beam fluence, irradiaton time, γ line intensity, etc., is obtained as discussed in [23]. The measured excitation functions are shown in figs. 1 to 11.

The uncertainty affecting the absolute values of the measured cross-sections is estimated to be about 25% at all energies due mainly to the uncertainty in the thickness of the target specified by Goodfellow and to a lesser extent to the uncertainty in the beam fluence, the measured HPGe efficiency, the electronic dead time, and statistical errors.

A preliminary theoretical analysis [24,25] of the excitation functions for production of residues in the interaction of ^{12}C with ^{103}Rh suggested that the near-target residues should be produced with the highest cross-sections. We speculated that the same could happen in the case of interaction of ^{16}O with ^{103}Rh. Unfortunately, the most important of these residues, those with mass 103, could not be identified in the experiments described above.

In fact, the measurement of the production cross-section of residues such as ^{103}Pd and ^{103m}Rh requires rather complex radiochemical procedures because they have very weak characteristic γ lines, thus, in order to achieve an accurate evaluation of their production cross-section, the measurement of the yield of the 20.074 and

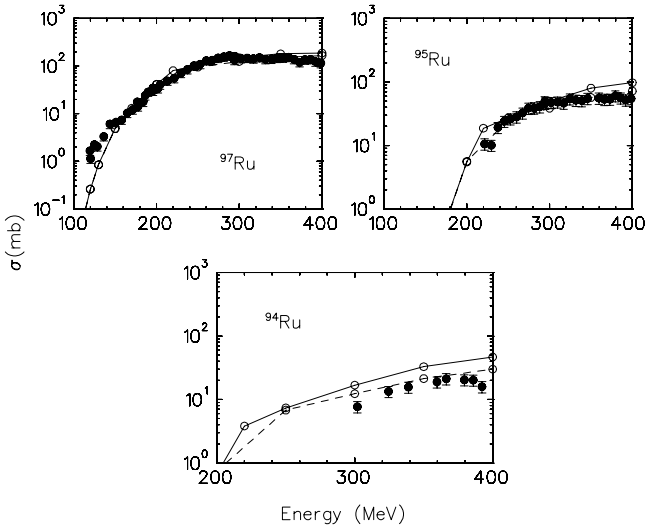

Fig. 8. Comparison of experimental (black dots) and calculated (open dots connected by the dashed and full lines) excitation functions for production of Ru isotopes. The assumptions underlying the two theoretical predictions are explained in the text.

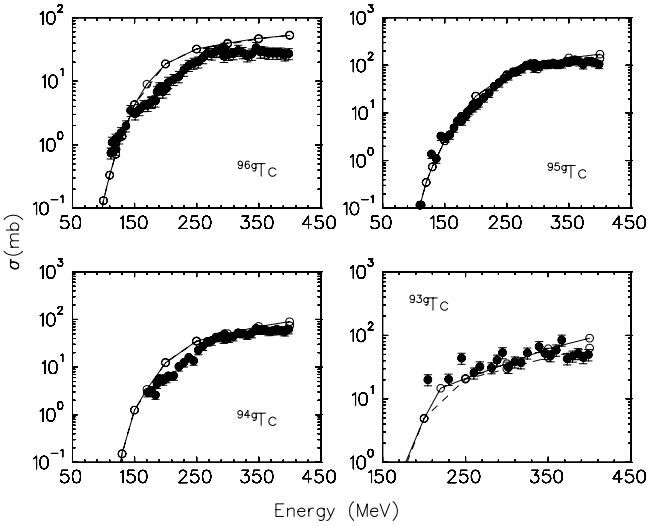

Fig. 9. Comparison of experimental (black dots) and calculated (open dots connected by the dashed and full lines) excitation functions for production of Tc isotopes. The assumptions underlying the two theoretical predictions are explained in the text.

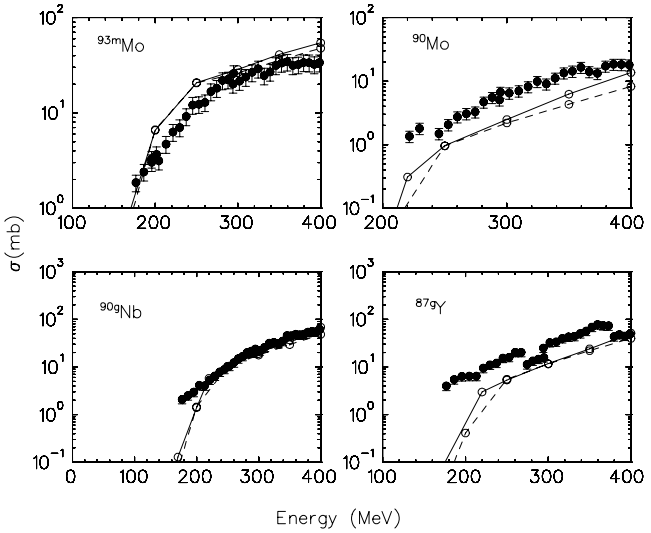

Fig. 10. Comparison of experimental (black dots) and calculated (open dots connected by the dashed and full lines) excitation functions for production of ^{93m}Mo, ^{90}Mo, ^{90g}Nb and ^{87g}Y. The assumptions underlying the two theoretical predictions are explained in the text.

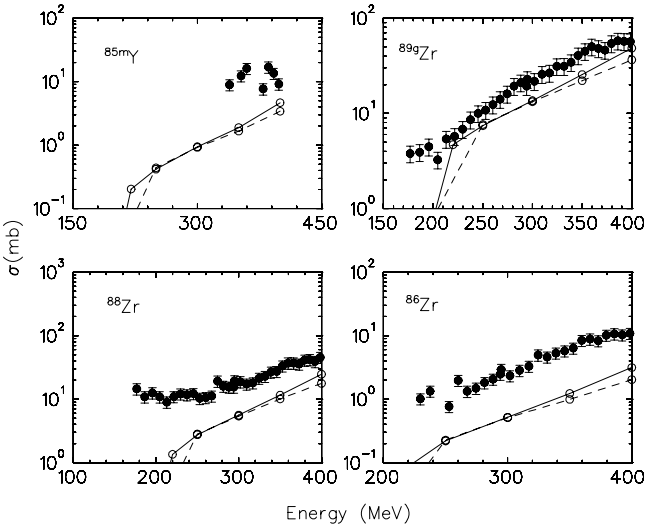

Fig. 11. Comparison of experimental (black dots) and calculated (open dots connected by the dashed and full lines) excitation functions for production of ^{85m}Y, ^{89g}Zr, ^{88}Zr and ^{86}Zr. The assumptions underlying the two theoretical predictions are explained in the text.

20.216 keV K_α X-rays is required. However, many other residues which may be produced in the considered two-ion interaction have X-ray lines with energies between 19 and 22 keV and thus a measurement of their production cross-section is not feasible without chemical separation. The other member of the isobaric multiplet, ^{103}Ru, has quite abundant γ lines, but its production cross-section was predicted to be very low, so, also in this case, chemical separation was advisable in order to make its γ lines visible above the quite intense background.

In an experiment especially designed to identify these residues, two tin disks of $RhCl_3 \cdot xH_2O$ (supplied by Strem Chemicals Inc., Newburyport, MA) were produced by pressing the powder in a punch-and-die set to a pressure of 20 bar. They had a 15 mm diameter and 79 mg/cm^2 thickness. The two disks were irradiated with a 393.6 MeV, 50 nA ^{16}O beam, the first for one hour to measure the production cross-section of the shorter-lived nuclides, the second for 5 hours to measure the cross-section of the longer-lived nuclides. In both cases the ^{16}O energy at the target half thickness was about 350 MeV. The experiment and the chemical separation technique are described in detail elsewhere [26]. The uncertainty of the measured

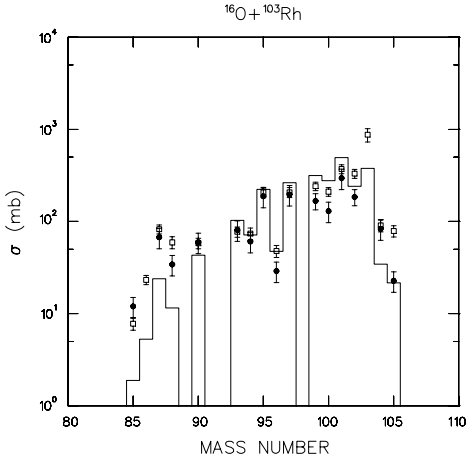

Fig. 12. Comparison of the yield of $85 \leq A \leq 105$ isobars produced in the interaction of oxygen ions of 350 MeV with ^{103}Rh as measured in [6] (open squares) and in the experiment here discussed (black dots) with that evaluated by subtracting, in complete-fusion processes, as discussed in the text, the initial energy loss from the projectile kinetic energy (full-line histogram). The observed isobars are given in parentheses: $A = 105$ (^{g}Ag), $A = 104$ (Cd and ^{g}Ag), $A = 103$ (^{g}Ag, Pd, ^{m}Rh, Ru), $A = 102$ ($^{m+g}$Rh), $A = 101$ (Pd and ^{m}Rh), $A = 100$ (Pd and $^{m+g}$Rh), $A = 99$ (Pd and $^{m+g}$Rh), $A = 97$ (^{g}Rh, Ru), $A = 96$ (^{g}Tc), $A = 95$ (Ru, $^{m+g}$Tc), $A = 94$ (^{g}Tc), $A = 93$ (^{g}Tc and ^{m}Mo), $A = 90$ (Mo and ^{g}Nb), $A = 88$ (Zr), $A = 87$ ($^{m+g}$Y), $A = 86$ (Zr and ^{g}Y), $A = 85$ (^{m}Y).

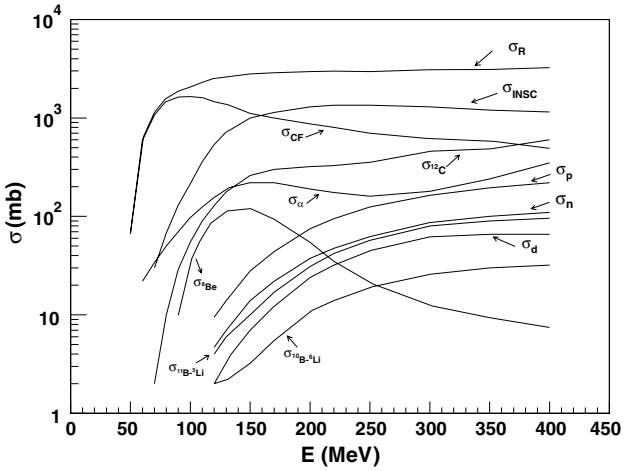

Fig. 13. Reaction cross-section, σ_R and cross-sections of the contributing reaction mechanisms ($\sigma_{\rm Cf}$ = complete fusion, $\sigma_{\rm INSC}$ = inelastic scattering, $\sigma_{^{12}\rm C}$ = incomplete fusion of one ^{12}C, $\sigma_{^{8}\rm Be}$ = incomplete fusion of a ^{8}Be, σ_α = incomplete fusion of one α-particle, $\sigma_{\rm p}$ = proton transfer, $\sigma_{\rm n}$ = neutron transfer, $\sigma_{\rm d}$ = deuteron transfer, $\sigma_{^{11}\rm B\text{-}^{5}Li}$ = incomplete fusion of a ^{11}B or a ^{5}Li, $\sigma_{^{10}\rm B\text{-}^{6}Li}$ = incomplete fusion of a ^{10}B or a ^{6}Li).

cross-sections was estimated to be about 15%. Figure 12 shows, as a function of residue mass number, the production cross-section of the more abundant isobars observed at a nominal energy of 350 MeV.

4 Theoretical analysis

In order to evaluate the production cross-section of a given residue one has to consider all the different reaction paths which may lead to its formation or to the formation of precursors which may decay to it. Due to its complexity, the analysis of the excitation functions alone without complementary information may introduce ambiguities in the interpretation of the data, which may partially cast doubt on any conclusions.

The calculations presented in this paper take advantage of the results of the experiments made to measure the IMF production cross-sections [5,7], which were briefly summarized above. The most relevant information concerns the binary fragmentation cross-sections of ^{16}O, whose values are obtained by extrapolation from those measured for the interaction of oxygen with ^{93}Nb, and the average loss of energy which, according to our interpretation, ^{16}O suffers before breaking-up.

The very succesful analysis of the excitation functions for residue production in the interaction of ^{12}C with ^{103}Rh was made assuming that after ^{12}C binary fragmentation, one fragment may be absorbed by the target nucleus, *i.e.*, a break-up–fusion mechanism. This assumption is also retained in the present calculations. Thus, the cross-section for fusion of one fragment is simply given by the cross-section for observation of the complementary *spectator* fragment deduced by the analysis of the measured IMFs spectra [5,7]. The break-up–fusion hypothesis allows one to evaluate also the excitation energy distributions and the recoil distributions of the nuclei produced by the fusion of the *participant* fragment once the spectra of the spectator fragment are known. These are evaluated by folding the LPWA spectra [13,14] with the projectile survival probability function, which satisfactorily reproduces the measured spectra [5,7].

In addition to break-up–fusion reactions, other processes which most presumably contribute to residue production are the complete fusion of the projectile and the target (for which we take the values given by [27]) and the inelastic-scattering cross-section, the value of which is assumed to be given by the difference between the reaction cross-section [27] and the sum of all the contributions previously mentioned.

These assumptions are summarized in fig. 13 which gives the cross-sections of all considered mechanisms as a function of the incident energy.

These assumptions and the recourse to experimental findings related to complementary data greatly reduce the degrees of freedom of the ensuing calculations. This is an enormous improvement with respect to previous analyses of this type. In fact, the only really free parameter in this part of the calculation is the one which gives the energy distribution of the inelastically scattered ions $P(E)$ for which, in agreement with the energy dependence of the projectile survival probability, we assume an exponential decrease with the scattered ion loss of energy $E_{\rm loss} = E_{\rm max} - E$, *i.e.*, $P(E) \propto \exp(-KE_{\rm loss})$. The value

of K was obtained by a best fitting of the excitation functions of near-target residues, to the formation of which inelastic-scattering reactions greatly contribute. At energies below about 150 MeV, the values of K which are deduced in this way are characterized by rather large uncertainties. However, there is a clear indication of a decrease of K with incident energy which leads to an almost constant value of about $0.02\,\mathrm{MeV}^{-1}$ at incident energies exceeding 200 MeV.

The nuclei produced by complete fusion and break-up–fusion reactions are in a state far from equilibrium. They are assumed to progress towards statistical equilibrium via a nucleon-nucleon interaction cascade which is simulated by a set of Boltzmann Master Equations (BMEs). The theory is discussed extensively in several articles (see [15, 16] and references therein) and therefore does not need to be repeated here. Here, we simply recall its basic assumptions. In BME theory one subdivides the states of the nucleon into bins characterized by constant values of Δp^2 (or $\Delta\epsilon$) and Δp_z, where p^2 and p_z are the square of the nucleon's momentum and the component of the momentum along the beam axis, respectively. The occupation probability of these bins, $n(\epsilon, \theta, t)$, which initially depends on the particular two-ion interaction, changes with time as a consequence of nucleon interactions (which may lead to a redistributions of the nucleons among different bins) and emission into the continuum of unbound nucleons and of nucleons which, if their momentum falls within a suitable sphere in momentum space, may coalesce into a cluster. These processes are characterized by their respective probabilities of occurrence per unit time (decay rates). The evolution with time of the occupation probability of each bin is calculated by solving a set of Boltzmann Master Equations (BMEs). The state occupation probability of nucleon aggregates formed by nucleon coalescence, $N_{\mathrm{C}}(E, \theta, t)$, in the course of the interaction cascade depends on $n(\epsilon, \theta, t)$ and the number and type of their nucleons. Once $n(\epsilon, \theta, t)$ and $N_{\mathrm{C}}(E, \theta, t)$ are known one may evaluate the ejectile spectra [15,16].

As mentioned above, these calculations very satisfactorily reproduce the experimental spectra of IMF emitted with energy around the Coulomb barrier, as shown, *e.g.*, in [5,7] and this result strengthens our opinion that the theory is reasonable.

In the case of α-particle incomplete fusion, both as single entities and/or as a part of a ^{8}Be fragment, another process taken into account is their re-emission, with a large fraction of their original energy after a few interactions with the target nucleons, as suggested by previous work on α-particle–induced reactions [28,29]. The probability of these events is evaluated as explained in [30].

At the end of the n-n interaction cascade which follows complete or incomplete fusion, nuclei in thermal equilibrium are created whose excitation energy and the A and Z distributions are evaluated by the theory. We also assume that the target nucleus excited by inelastic scattering should be in a state of thermal equilibrium. The subsequent decay of these equilibrated nuclei by particle evaporation (evaluated by rather standard techniques [31]) leads to the observed residues.

Unfortunately, the complete calculation, to be tractable, requires a number of approximations which may carry some bias onto the numerical results. One of these approximations concerns the Monte Carlo simulation of pre-equilibrium emissions from systems created in incomplete-fusion events. In this case the energy and angular dependence of the spectra of the light particles emitted in the course of the n-n interaction cascade is assumed to be equal to that of the spectra evaluated by BME theory for complete-fusion reactions, and their absolute value is simply scaled by the ratio of the mass of the absorbed fragment to the mass of the projectile. This is a very good approximation in the case of single-nucleon emission but becomes progressively worse with increasing emitted particle mass. The correct evaluation of the pre-equilibrium particle spectra for each fusing fragment with each possible energy implies an enormous increase of computing time which, up to now, we have been unable to confront. For the same reason, we neglect in break-up–fusion processes the quite considerable emission of IMFs produced by nucleon coalescence.

Figures 1 to 11 show the comparison of the data (full dots) and the theoretical predictions made with the procedure outlined above (dashed lines).

Even if the qualitative features of all the excitation functions are satisfactorily reproduced and in most of the cases also their absolute value, in a few cases the theory does not reproduce accurately the excitation function at the highest energies. We wish to suggest here how many of these dicrepancies may be eliminated.

As we have recalled above, according to our theoretical approach, before breaking up the projectile may lose a not negligible fraction of its energy. In our model, this energy is assumed to excite quite low-energy states of the target nucleus. We assume that once the participant fragment fuses with the target nucleus, its nucleons initiate the cascade of n-n collisions interacting with the target nucleons. The target nucleons which have been slightly excited in the initial interactions do not really contribute to the emission of fast particles in the thermalization stage and their energy is assumed to contribute to the excitation energy of the equilibrated nuclei which are eventually produced.

In our previous calculations a similar effect was not considered in the complete-fusion process at energies above about 10 MeV/n. In fact, below this energy, we assume that when the projectile and the target nucleons start to interact, the relative translational momentum of the two ions is greatly reduced by their Coulomb repulsion and a sizeable fraction of the energy (equal to the two-ion Coulomb barrier at contact) is *frozen* as collective deformation energy. At the end of thermalization this energy transforms into chaotic thermal energy of the nucleons of the equilibrated nucleus left. This assumption proved essential to reproduce the tails of the observed excitation functions at these low incident energies in the interaction of ^{12}C with heavy nuclei such as ^{181}Ta and

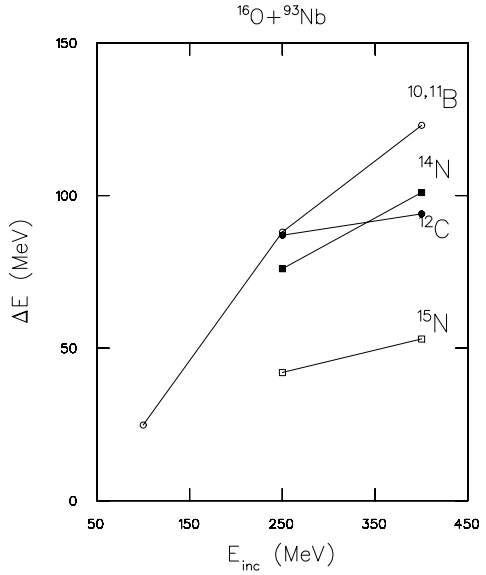

Fig. 14. Average energy loss of ^{16}O, before fragmentation, producing the indicated fragments, as a function of the incident energy [5,7].

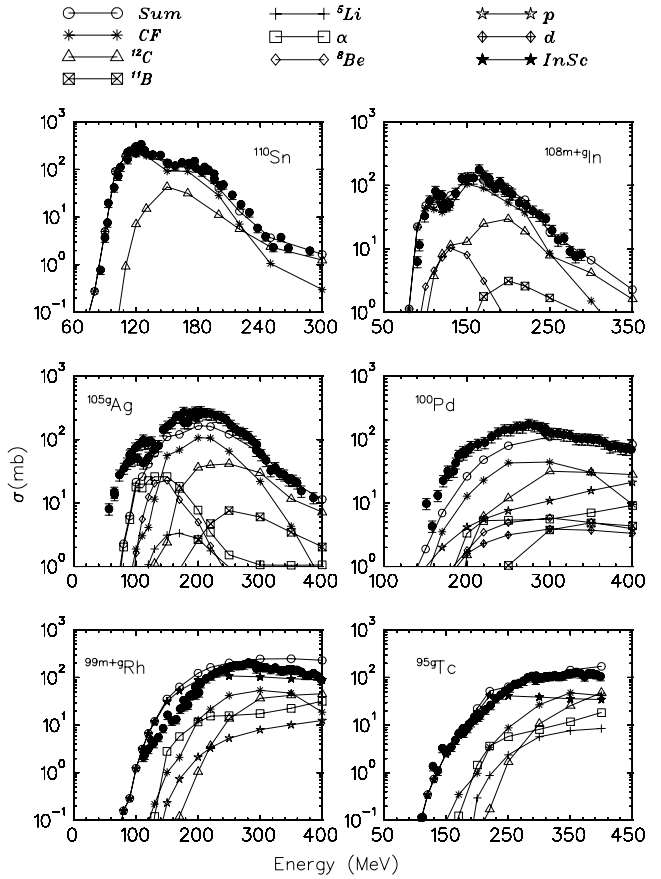

Fig. 15. Mechanisms contributing to the formation of a few representative residues.

^{197}Au [10,23] and ^{103}Rh [6,32] and ^{16}O with heavy nuclei such as ^{165}Ho and ^{181}Ta [10,23]. With increasing energy above 10 MeV/n, the effect was assumed to disappear in complete-fusion processes and all the projectile kinetic energy was considered in evaluating the cascade of n-n interactions (above 20 MeV/n it was also increased to account for the increased depth of the composite nucleus potential well as compared to those of the projectile and the target [33]). This was made with the presumption that the initial energy loss is a part of the process (simulated by the cascade of n-n interactions) through which the two-ion kinetic energy transforms into random thermal energy.

However, in analysing the present data we found that the reproduction of quite a number of excitation functions was noticeably improved by subtracting in complete-fusion reactions the energy lost by the projectile while approaching the target from the kinetic energy of the projectile nucleons and assuming it to contribute to the excitation energy of equilibrated nuclei produced at the end of the n-n interaction cascade. In this assumption the initial interaction heats the target nucleus and partly inhibits the emission of fast particles and particle aggregates during thermalization which, nevertheless, remains crucial for reproducing the energy dependence of many excitation functions at the highest incident energies. Due to the greater excitation energy of equilibrated nuclei at the end of thermalization there is a considerable increase of the multiplicity of the evaporated particles and a decrease of the ratio of fast to low particles emitted during the nuclear de-excitation of the nuclei formed in the two-ion interaction. The result critically depends on the initial energy loss in complete-fusion events. The estimate of this quantity is difficult because the average energy loss before fragmentation, as deduced from the analysis of the IMF spectra [5,7], seems to depend, as shown in fig. 14, on the particular fragmentation of ^{16}O, as it is also found in the case of ^{12}C induced reactions [8] with estimates numerically consistent with those used in this paper for ^{16}O.

In figs. 1 to 11 the full lines represent the results of calculations made by assuming that in complete-fusion reactions, which correspond to the most central collisions, at incident energies above 200 MeV, the initial energy loss of the projectile which contribute to the equilibrated nucleus excitation energy should be about one half of the projectile energy. In fig. 12 the experimental cross-sections for production of residues of mass $85 \leq A \leq 105$ measured in the interaction of ^{16}O with ^{103}Rh at 350 MeV incident energy in this work and in [26] are compared with the theoretical predictions made with the same hypothesis (full-line histogram). Although the improvement is very impressive in some cases, we nevertheless feel that in complete-fusion reactions the subdivision of the projectile energy into thermal energy given to the target nucleus in the initial interaction and orderly kinetic energy starting the n-n interaction cascade is still an open problem requiring further studies especially investigating the influence of this assumption on the analysis of the data which we have considered in our previous works where we did not find any clear evidence for a similar effect [5–9].

As one clearly sees, most of the excitation functions are reproduced with remarkable accuracy, which is in

fact comparable and in some cases even better than that achieved in the analysis of the excitation functions of nucleon-induced reactions [34]. This is a very rewarding result if one considers both the much greater complexity of a heavy-ion interaction and the fact that most of the parameters we used in the calculations are given *a priori* and are those that very satisfactorily reproduce the IMF spectra measured in separate experiments [5,7].

In the lowest-energy region the excitation functions of the heaviest residues are clearly structured. This happens when a few mechanisms contribute to the formation of a given residue. The tails of these excitation functions show the prominent role of incomplete-fusion events.

With increasing energy the less-structured shape of the excitation functions reflects the contribution of many different reaction paths.

It is instructive to follow in fig. 15 how the contributions of the reaction mechanisms considered evolve with decreasing mass of the residue in a few representative cases.

There is only one systematic disagreement between the data and the theoretical results. It concerns the prediction of the cross-sections for production of the lighter residues (those farther removed from the target nucleus, such as the Zr and Y isotopes) in the threshold energy region. For some of these nuclei, as found in the same energy range also by [6] in the case of the interaction of ^{12}C with ^{103}Rh, the calculated threshold is substantially higher than the observed one. The excitation functions of these residues are quite noticeably underestimated. As in the case of ^{12}C-induced reactions there is some indication that with increasing energy the discrepancy is partially removed. Thus, as in the case of ^{12}C-induced reactions the disagreement might not indicate an intrinsic deficiency of the theoretical approach, but might be a consequence of some of our approximations.

5 Summary and conclusion

As in the case of the reactions induced by ^{12}C on ^{103}Rh at incident energies of a few tens of MeV/n we have shown that it is possible to give a comprehensive account of the reactions which may occur in the interactions of ^{16}O with a medium mass nucleus such as ^{103}Rh.

In our model the considered reaction mechanisms, such as projectile fragmentation and nucleon coalescence, weakly depend on the target nucleus mass and charge, thus we expect that calculations of this kind have a reliable predictive ability and may satisfactorily predict the cross-sections of reactions induced by ^{16}O on nuclei of widely different mass. A clear indication of this is afforded by the comparison of the cross-sections for incomplete-fusion reactions given in [10] for the interaction of ^{16}O with ^{181}Ta with those shown in fig. 13 for the interaction of ^{16}O with ^{103}Rh. In spite of some differences in the theoretical interpretation of the data (in [10] the contribution of inelastic scattering was not considered, the importance of which was only recognized in later studies) the energy dependence and the absolute values of the cross-sections for CF, ^{12}C, α-particle and ^{8}Be incomplete fusion appear to be similar and the differences found may be attributed to Coulomb effects due to the considerably higher charge of ^{181}Ta in comparison with ^{103}Rh.

The experiments and the ensuing theoretical analysis which we have discussed in this paper were made not only to increase our knowledge of the reaction mechanisms but also for helping to meet the demands coming from applications and interdisciplinary fields which always require a comprehensive information on the reactions which may occur in a nuclear interaction. The quantitative results that we have obtained indicate that our investigation should indeed be useful for this purpose.

In the course of the years we benefitted from the invaluable help of many colleagues and students. Among the colleagues to whom we are deeply indebted we must mention Drs. Steve Mills, Meiring Nortier, Nico van der Walt and Khosro Aardaneh of iThemba LABS, Prof. J.P.F. Sellschop of Schonland Research Centre, Profs. Enrica Gadioli Erba, Claudio Birattari, Michela Cavinato, and Elsa Fabrici of Milan University. Among the students, Trevor Stevens of Schonland Research Centre, Mara Bello, Gianfranco Bello and Francesca Albertini of Milan University.

References

1. R.H. Haight, M.B. Chadwick, T. Kawano, P. Talou (Editors), *Proceedings of the International Conference on Nuclear Data for Science & Technology, Santa Fe, Sept. 26 - Oct. 1, 2004*, AIP Conf. Proc. **769** (2005).
2. *Nuclear Data for Neutron and Proton Radiotherapy and Radiation protection*, ICRU Report 63 (2000).
3. U. Amaldi, Nucl. Phys. A **751**, 409c (2005).
4. F. Ballarini, G. Battistoni, F. Cerutti, A. Fassò, A. Ferrari, E. Gadioli, M.V. Garzelli, A. Mairani, A. Ottolenghi, H.G. Paretzke, V. Parini, M. Pelliccioni, L. Pinsky, P.R. Sala, D. Scannicchio, S. Trovati, M. Zankl, *Advances in Space Research* (2006), in press, available on the web.
5. E. Gadioli, G.F. Steyn, F. Albertini, C. Birattari, M. Cavinato, S.H. Connell, A.A. Cowley, E. Fabrici, S.V. Förtsch, E. Gadioli Erba, J.J. Lawrie, M. Pigni, J.P.F. Sellschop, E. Sideras Haddad, Eur. Phys. J. A **17**, 195 (2003).
6. E. Buthelezi, F. Cerutti, E. Gadioli, G.F. Steyn, S.H. Connell, A.A. Cowley, Nucl. Phys. A **753**, 29 (2005).
7. E. Gadioli, G.F. Steyn, C. Birattari, C. Catarisano, M. Cavinato, S.H. Connell, A.A. Cowley, E. Fabrici, S.V. Förtsch, E. Gadioli Erba, J.J. Lawrie, J.P.F. Sellschop, E. Sideras Haddad, Nucl. Phys. A **708**, 391 (2002).
8. B. Becker, F. Albertini, E. Gadioli, G.F. Steyn, M. Cavinato, S.H. Connell, A.A. Cowley, E. Fabrici, S.V. Förtsch, E. Gadioli Erba, J.J. Lawrie, E. Sideras Haddad, Eur. Phys. J. A **18**, 639 (2003).
9. L.J. Mudau, F. Cerutti, E. Gadioli, A. Mairani, S.V. Fortsch, E.Z. Buthelezi, G.F. Steyn, S.H. Connell, J.J. Lawrie, R. Neveling, F.D. Smit, E. Sideras Haddad, Nucl. Phys. A **761**, 190 (2005).
10. E. Gadioli, Acta Phys. Pol. B **30**, 1493 (1999).

11. E. Gadioli, M. Cavinato, E. Fabrici, E. Gadioli Erba, R. Bassini, C. Birattari, S. Crippa, G.F. Steyn, S.V. Förtsch, J.J. Lawrie, F.M. Nortier, S.H. Connell, E. Sideras Haddad, J.P.F. Sellschop, A.A. Cowley, Eur. Phys. J. A **8**, 373 (2000).
12. E. Gadioli, G.F. Steyn, C. Birattari, M. Cavinato, S.H. Connell, A.A. Cowley, E. Fabrici, S.V. Förtsch, E. Gadioli Erba, J.J. Lawrie, F.M. Nortier, J.P.F. Sellschop, E. Sideras Haddad, Eur. Phys. J. A **11**, 161 (2001).
13. K.W. McVoy, Carolina Nemes, Z. Phys. A **295**, 177 (1980).
14. S.L. Tabor, L.C. Dennis, K. Abdo, Phys. Rev. C **24**, 2552 (1981).
15. M. Cavinato, E. Fabrici, E. Gadioli, E. Gadioli Erba, E. Risi, Nucl. Phys. A **643**, 15 (1998).
16. M. Cavinato, E. Fabrici, E. Gadioli, E. Gadioli Erba, G. Riva, Nucl. Phys. A **679**, 753 (2001).
17. J. Blachot, G. Marguier, Nucl. Data Sheets **66**, 451 (1992).
18. J. Blachot, G. Marguier, Nucl. Data Sheets **73**, 81 (1994).
19. J. Blachot, G. Marguier, Nucl. Data Sheets **67**, 1 (1992).
20. J. Blachot, G. Marguier, Nucl. Data Sheets **75**, 739 (1995).
21. J. Blachot, Nucl. Data Sheets **84**, 277 (1998).
22. R.D. Evans, *The Atomic Nucleus* (McGraw-Hill, New York, 1955).
23. M. Cavinato, E. Fabrici, E. Gadioli, E. Gadioli Erba, P. Vergani, M. Crippa, G. Colombo, I. Redaelli, M. Ripamonti, Phys. Rev. C **52**, 2577 (1995).
24. E. Gadioli, C. Birattari, M. Cavinato, E. Fabrici, E. Gadioli Erba, V. Allori, C. Bovati, F. Cerutti, A. Di Filippo, E. Galbiati, T. Stevens, S.H. Connell, J.P.F. Sellschop, S.J. Mills, F.M. Nortier, G.F. Steyn, C. Marchetta, Phys. Lett. B **394**, 29 (1997).
25. E. Gadioli, C. Birattari, M. Cavinato, E. Fabrici, E. Gadioli Erba, V. Allori, F. Cerutti, A. Di Filippo, S. Vailati, T. Stevens, S.H. Connell, J.P.F. Sellschop, F.M. Nortier, G.F. Steyn, C. Marchetta, Nucl. Phys. A **641**, 271 (1998).
26. E.Z. Buthelezi, K. Aardaneh, G.F. Steyn, E. Gadioli, T.N. Van der Walt, F. Albertini, F. Cerutti, S.H. Connell, A.A. Cowley, F.M. Nortier, J. Radiat. Nucl. Chem. **258**, 649 (2003).
27. W.W. Wilcke, J.R. Birkelund, H.J. Wollersheim, A.D. Hoover, J.R. Huizenga, W.U. Schröder, L.E. Tubbs, At. Data Nucl. Data Tables **25**, 389 (1980).
28. E. Gadioli, E. Gadioli Erba, Z. Phys. A **299**, 1 (1981).
29. E. Gadioli, E. Gadioli Erba, M. Luinetti, Z. Phys. A **321**, 10 (1985).
30. E. Gadioli, M. Cavinato, E. Fabrici, E. Gadioli Erba, C. Birattari, I. Mica, S. Solia, G.F. Steyn, S.V. Förtsch, J.J. Lawrie, F.M. Nortier, T.G. Stevens, S.H. Connell, J.P.F. Sellschop, A.A. Cowley, Nucl. Phys. A **654**, 523 (1999).
31. P. Vergani, E. Gadioli, E. Vaciago, E. Fabrici, E. Gadioli Erba, M. Galmarini, G. Ciavola, C. Marchetta, Phys. Rev. C **48**, 1815 (1993).
32. C. Birattari, M. Bonardi, M. Cavinato, E. Fabrici, E. Gadioli, E. Gadioli Erba, F. Groppi, M. Bello, C. Bovati, A. Di Filippo, T. Stevens, S.H. Connell, J.P.F. Sellschop, S.J. Mills, F.M. Nortier, G.F. Steyn, C. Marchetta, Phys. Rev. C **54**, 3051 (1996).
33. C. Brusati, M. Cavinato, E. Fabrici, E. Gadioli, E. Gadioli Erba, Z. Phys. A **353**, 57 (1995).
34. E. Gadioli, P.E. Hodgson, *Pre-equilibrium Nuclear Reactions* (Oxford Science Publications, Clarendon Press, Oxford, 1992).